VOLUMES AND ORIENTATION OF SECONDARY POROSITY IN THE BURNS FORMATION, MERIDIANI PLANUM, MARS. S. M. Perl[1], S. M. McLennan[1], J. P. Grotzinger[2], K. E. Herkenhoff[3], and the Athena Science Team, [1]Department of Geosciences, State University of New York, Stony Brook, NY 11794-2100 (Scott.Perl@stonybrook.edu); [2]Division of Geological and Planetary Sciences, California Institute of Technology, Pasadena, CA 91125; [3]United States Geological Survey, Astrogeology Team, Flagstaff, AZ, 86001.

Introduction: Development of secondary porosity occurs post-depositionally in sedimentary rocks during mineral transformation, rock fracture, and mineral dissolution. The timing and shape of secondary pores provide constraints on the record of fluid flow through sedimentary rocks. For comparison, in terrestrial carbonate rocks, secondary porosity, where present, typically is in the range of 5-15% by volume whereas in sandstones it may reach 15-30% [1].

Sedimentary rocks studied by the *Opportunity* rover reveal evidence of diagenetic processes including formation of hematite spherules, recrystallization, crystal molds, and others. McLennan et al. [2] noted the presence of void spaces within the Burns formation that were interpreted as secondary porosity formed by dissolution of soluble salts during groundwater recharge.

The purpose of this study is to quantify the volumes, sizes, and spatial orientations of secondary pores and evaluate if there is any relationship with the type of secondary porosity.

Secondary Porosity Classification: Three types of secondary porosity have been identified (Fig. 1): crystal moldic porosity (typically fabric selective), sheet-like to elongated vug, or channel porosity (typically non-fabric selective), and a modified (enlarged) version of both.

Crystal Mold Porosity: One of the first diagenetic textures recognized in the Burns formation were mm-sized "vugs", noted by Squyres, et al. [4]. Using the porosity classification of Choquette and Pray [1], these are more precisely termed crystal moldic porosity. The average size of these pores have a width of 1 (s.d.=0.5) mm and a length of 5 (s.d.=3) mm. and their tabular shape suggests the former presence of a monoclinic mineral. The amount of crystal mold porosity has been found to vary considerably from place to place. These pores have been interpreted to represent dissolution of a highly soluble mineral such as Mg-sulfates, ferrous sulfates or chlorides [2,4].

Elongated to Sheet-like Vug and Channel Porosity: These pore types are related and occur in patterns that appear to both parallel and cut across bedding. Choquette and Pray [1] define channel porosity as non-fabric selective secondary porosity where length to width ratios are greater than ten. Many of the pores observed in the Burns formation are elongate but have length to width ratios less than ten. Although many of these vugs cut across primary bedding fabrics, in many places they also appear to preferentially align along bedding thus giving them a mixed fabric selective – non-fabric selective character. Accordingly, these have been termed elongate to sheet-like vugs. They are interpreted to represent dissolution of relatively soluble mineral phase(s) such as Mg-sulfates [2].

Pore Modification: Although less common we have observed the presence of significantly enlarged pores. These oversized vugs are considerably larger than the size of regular vugs and are found to modify each of the two types of secondary porosity. The amount of modification varies from rock to rock. The process of pore modification occurs mostly within cm- to dm-scale stratigraphic zones in the upper part of the Burns formation, notably in the vicinity of the Whatanga contact separating the middle and upper units [3]. Within the Karatepe stratigraphic section in Endurance crater, the rock targets Virginia and Grindstone contain these enlarged pores as well as southeast of Burns Cliff at the target Wharenhui. These zones have been interpreted to represent diagenetic fronts associated with the presence of a stagnant paleowater table [2,3].

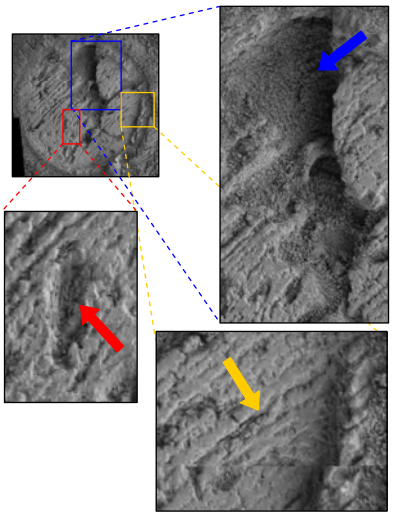

Fig. 1: MI mosaic of RATed surface Virginia and images showing examples of elongate to sheet-like porosity (yellow arrow), crystal moldic porosity (red arrow), and an example of a modified pore (blue arrow).

Analysis: To measure secondary porosity of these rocks we have used MI mosaics of RATed surfaces (Fig. 2). Although numerous RAT surfaces have been produced in the Burns formation for chemical and Mössbauer measurements, for textural studies we are limited to surfaces where microtextures have not been

obscured by abundant fine grained debris produced during the RAT procedure.

Volumes of secondary porosity: Our analysis of pore areas is based on a threshold technique where areas identified as secondary porosity are enhanced as green (Fig. 2). This approach also results in some non-pores being mis-identified (notably spherules). Careful visual comparison between original MI mosaics, false color equivalents, and digital elevation models (Fig. 3) allows for manual subtraction of these regions. Further editing includes removal of RAT margins and other features that are clearly not porosity. In some cases, shadowed regions are also mis-identified and for these, brightness and contrast levels are manipulated to obtain appropriate threshold levels. In some cases, the threshold method was unable to differentiate between pores and non-pores and these areas were excluded from consideration. It should also be noted that our calculated values are most likely lower limits due to the possible filling of RAT tailings into the abraded hole and that we assume that areal distribution of secondary porosity equates to volume.

Our estimates of secondary porosity volumes are presented in the table below. Secondary porosity varies between about 15-40%. Rocks with well-developed oversized pores not surprisingly have the highest pore volumes but the increase in pore volumes does not appear to be that great. The single sample measured in the Erebus crater region (Strawberry) has significantly less secondary porosity. This may be due to the RATed target lying close to the bedding plane while other targets are more orthogonal to bedding.

Cobble Hill	33.4%	Endurance Crater
Virginia	31.6%	Endurance Crater
London	29.9%	Endurance Crater
Grindstone	33.8%	Endurance Crater
Drammensfjorden	24.6%	Endurance Crater
Paikea	32.8%	Endurance Crater
Wharenhui	41.4%	Endurance Crater
Strawberry	15.8 %	Erebus region

Type, size and orientation of secondary pores: The length, width and orientation (relative to bedding) are being measured in order to evaluate any distinctions in size or distributions between the three types of secondary porosity. The selection of pores used for measurement is determined systematically by a grid overlaying the original MI mosaic. The majority (~80%) of the secondary porosity is of elongated/channel type with fewer occurrences of crystal molds (~8%).

The analysis of Cobble Hill has a generally uniform pattern of secondary porosity distribution (Fig. 4). Most of the pores follow an orientation between -10° and +10° with length to width ratios between 2 and 20. The pores that are inclined to bedding (<-10°;>+10°) mostly have length to width ratios less than 2.

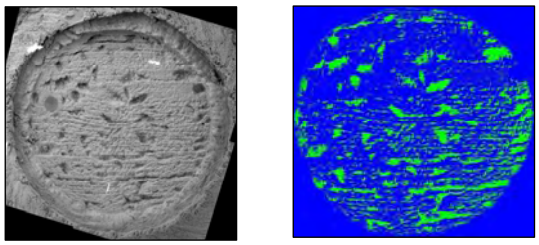

Fig. 2: Original MI mosaic of London (left) and its thresholded image (right). This method enhances regions that may not be porosity (i.e., concretions, RAT outer margin). These regions are digitally removed before the overall secondary porosity is calculated.

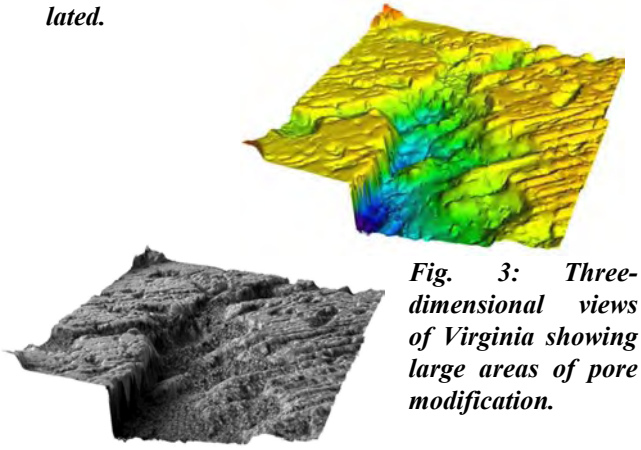

Fig. 3: Three-dimensional views of Virginia showing large areas of pore modification.

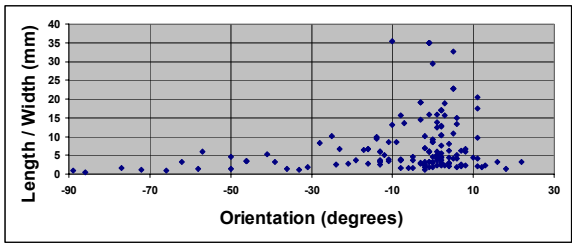

Fig. 4: Pore volume measurements of Cobble Hill (n=166). The majority of pores are parallel to bedding (-10° - +10°) while 21% of the pores are inclined to the bedding.

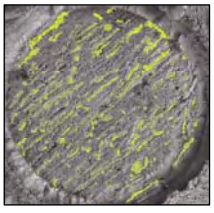

References: [1] Choquette, P. W. and Pray, L. C. (1970) Am. Assoc. Pet. Geol. Bull. 54, 207-250. [2] McLennan, S. M., et al., (2005) EPSL, 240, 95-121. [3] Grotzinger, J. P., et al. (2005) EPSL, 240, 11-72. [4] Squyres, S. W., et al. (2004) Science, 306, 1709– 1714.